

Multi-Objective Logarithmic Extremum Seeking for Wind Turbine Power Capture with Load Reduction

Devesh Kumar¹, Nicholas Gans² and Mario A. Rotea³

Abstract—This paper describes a multi-objective ESC strategy that determines Pareto-optimal control parameters to jointly optimize wind turbine loads and power capture. The method uses two optimization objectives calculated in real time: (a) the logarithm of the average power and (b) the logarithm of the standard deviation of a measurable blade load, tower load or the combination of these loads. These two objectives are weighted in real-time to obtain a solution that is Pareto optimal with respect to the power average and the standard deviation of chosen load metric. The method is evaluated using NREL FAST simulations of the 5-MW reference turbine. The results are then evaluated using energy capture over the duration of the simulation and damage equivalent loads (DEL) calculated with MLife.

I. INTRODUCTION

When a wind turbine operates below its rated wind speed (region 2) the power output is proportional to the power available in the wind and the parameter of proportionality is the so-called power coefficient C_p . For variable-speed variable-pitch wind turbines, C_p is a unimodal function of the blade pitch angle (β) and tip speed ratio (λ) [1], which means that there is an optimal blade pitch angle and tip speed ratio to achieve the maximum C_p and therefore, maximum output power. The optimal value of tip-speed ratio and blade-pitch angle may differ from turbine to turbine due to complex aerodynamic site specific effects and other factors. Moreover, these optimal values also change with time due to wear and tear of blade surface, changes in ambient conditions, etc.

Extremum Seeking Control (ESC) has emerged as a useful, model-free, real-time optimization strategy to optimize wind turbine power output despite uncertainty and/or variations in C_p . Creaby *et al.* [2] studied ESC-based region-2 control with power feedback for rotor torque, blade pitch and yaw input. Field test results of ESC-based region-2 controllers on the NREL CART3 turbine were reported by Xiao *et al.* in [3]. In spite of the demonstrated success of ESC studies, a drawback of these strategies is the inconsistent and slow convergence behavior under changes in wind speed within region 2. Rotea [4] analyzed the root cause of inconsistent convergence and proposed a “log-power feedback” strategy for ESC-based wind turbine control, which was validated

with a simple reduced order model. Later, Ciri *et al.* [5] demonstrated, through high-accuracy, large eddy simulations, that the log-power feedback ESC calibrated at a given wind speed exhibits consistent and robust performance across all wind speeds within region 2 under realistic turbulent wind conditions.

The maximization of power in off-design conditions may have unintended consequences, such as an increase in aeromechanical loads on the blades and the turbine structure. Xiao *et al.* [6] proposed a multi-objective ESC for wind turbines with a single performance index combining the power and load objectives using pre-defined weights for the load and power objectives. Simulation results with the CART3 turbine model in FAST showed promising results.

In the current work, we propose a log-feedback, real-time weighted, multi-objective ESC algorithm for wind turbines. The performance index for the power objective (objective to be maximized) is the logarithm of the rotor power scaled by rated power, while the logarithm of standard deviation of the load moments, scaled by its running mean, is used as the performance index for the load objective function (objective to be minimized). The tunable turbine parameters are region-2 generator torque gain (k_t) and blade pitch angle (β). The real-time weighting seeks the shortest path to the Pareto front of the power and load objectives. Three different load objective are studied here: (1) Tower Base Fore-aft Bending Moment (TBFABM), (2) Blade Root Flap-wise Bending Moment (BRFWBM), and (3) combination of (1) and (2). FAST simulations on NREL 5MW turbine model demonstrate the effectiveness of the proposed approach.

Our preliminary study shows that the algorithm can achieve significant levels of load reductions, relative to log-power-feedback only ESC, with little to no change in energy capture. A contribution of this paper is the use of an update rule to determine real-time weights in order to achieve Pareto optimality in the power and loads optimization objectives.

The rest of the paper is organized as follows. Design guidelines for ESC, logarithmic feedback and multi-objective ESC are introduced in Section II. Section III has detailed discussion of the method adopted and ESC parameter design. Results are discussed in Section IV and conclusions can be found in Section V.

II. EXTREMUM SEEKING CONTROL (ESC)

A. ESC principles and design guidelines

A model-free, real-time optimization technique like ESC can optimize the performance of a nonlinear plant by searching for the unknown and/or time-varying input parameter

*This material is based upon work partially supported by the National Science Foundation under Grant No. 1728057

¹Department of Electrical and Computer Engineering, Center for Wind Energy, The University of Texas at Dallas, Richardson, TX 75080 USA

²The University of Texas at Arlington Research Institute, The University of Texas at Arlington, Arlington, TX 76019 USA

³Department of Mechanical Engineering, Center for Wind Energy, The University of Texas at Dallas, Richardson, TX 75080 USA
Correspondance: rotea@utdallas.edu

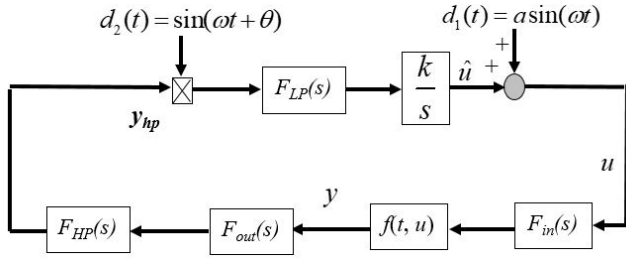


Fig. 1. Conventional ESC.

u^* that optimizes a selected performance index $f(u)$. A single-input single-output periodic perturbation based ESC strategy to extract the gradient information is shown in Figure 1. $F_{in}(s)$ and $F_{out}(s)$ are unity-gain, linear time-invariant (LTI) approximations of the input and output dynamics, respectively, and $y = f(t, u)$ denotes a possibly time-varying static map of the nonlinear plant. The online gradient estimation of ESC operation is based on applying a periodic dither $d_1(t) = a \sin \omega t$ and demodulation signal $d_2(t) = \sin(\omega t + \theta)$, where a is the dither amplitude, ω is the dither frequency and θ is the phase compensation. The high-pass filter $F_{HP}(s)$ is applied to the performance index y that aims to optimize (maximize/minimize) by tuning the input u . The low-pass filter $F_{LP}(s)$ with an integrator and gain k completes the ESC loop. The input u to the plant results from the perturbation by the dither, i.e. $u = \hat{u} + a \sin \omega t$. As for the plant output, the gradient is carried in the dither harmonic component. High-pass filtering of the output can remove the DC component; after which, multiplication by the demodulation signal can shift the gradient content to the DC. Application of the low-pass filter retains the gradient estimate at DC. Closing the loop with integral control can drive the gradient to 0 at steady state, provided that the averaged system is asymptotically stable, which implies that the optimum input u^* is reached. The standard ESC design guidelines [7] have been adopted in this study.

B. Conventional ESC with log-of-power feedback

Rotea [4] performed an analysis for ESC-based, Region-2 wind turbine control, which justifies the advantages of using logarithmic power feedback over power feedback under different wind speeds. The power contained in incoming wind of velocity is given by

$$P_{\text{wind}} = \frac{1}{2} \pi R^2 \rho V^3 \quad (1)$$

where, ρ is air density in kg/m^3 , R is rotor radius in m, and V is the incoming wind speed perpendicular to the rotor plane in m/s. The rotor power produced can then be given by

$$P = P_{\text{wind}} C_p(u) \quad (2)$$

where, C_p denotes the power coefficient of wind turbine, and u is a manipulated input such as the generator torque (or equivalently torque gain), blade pitch angle or yaw measurement. With the rotor power used as the performance index for ESC, its gradient with respect to u is

$$\frac{\partial P}{\partial u} = P_{\text{wind}} \frac{\partial C_p(u)}{\partial u} \quad (3)$$

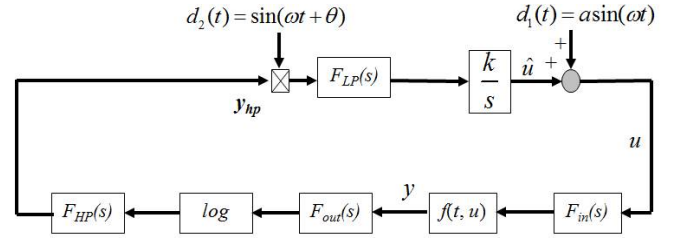


Fig. 2. Conventional ESC with log-power feedback.

which depends on the wind speed. For a gradient search algorithm like ESC, a wind speed dependent gradient yields a wind speed dependent convergence rate. This explains why the appropriate gain has to be tuned under different wind speeds. In contrast, if the logarithmic power is used as the performance index, i.e. $J = \ln P$, the gradient becomes

$$\frac{\partial J}{\partial u} = \frac{\partial}{\partial u} \ln(P_{\text{wind}} C_p(u)) = \frac{1}{C_p(u)} \frac{\partial C_p(u)}{\partial u} \quad (4)$$

which is independent of the wind speed. Therefore, the ESC process thus designed will be less affected by wind speed fluctuation. Rotea [4] demonstrated the effectiveness of this log-power feedback ESC with a Simulink-based simulation study. This idea from [4] is patent pending [8]. A typical conventional ESC with log power feedback is shown in Figure 2.

C. Multi-objective ESC with log-feedback

A multi-objective optimization (MOO) problem generally consists of a number of conflicting objective functions. Here, a real-time weighting selection algorithm is employed to obtain the optimal weights for the multi-objective extremum seeking control problem of wind turbines. Kumar and Gans [9] presented a real-time weighted multi-objective algorithm, in which they employed an extra inner loop ESC to determine the weights for multi-objective optimization in real-time. Results with static functions showed the promise of real-time weighting. This method employed the Multiple Gradient Descent Algorithm (MGDA) proposed in [10]. Since the extra inner loop will introduce an extra perturbation in the wind turbine system, the real-time weighted multi-objective algorithm is modified in this work and is discussed in detail in section III.

Conventionally, ESC is employed to maximize the output power in Region-2 operation of wind turbines by operating the wind turbine under optimal torque and pitch conditions. Extracting maximum power in off-design conditions can lead to higher mechanical loads on these structures, which will reduce the lifetime operation of these turbines. Therefore, conflicting objectives of power and mechanical loads can be used as optimizing functions in the multi-objective framework for wind turbines with optimizing variables as torque gain (k_t) and blade pitch (β). A detailed explanation on the implementation is presented in the next section. We make two assumptions here. The first is that the load cost function is convex. Under this assumption, the Pareto optimality condition is given by

$$\alpha \frac{\partial P}{\partial x} + (1 - \alpha) \frac{\partial L}{\partial x} = 0 \quad (5)$$

where P is the output power from wind turbine, L is the mechanical load being optimized, with x_1 as torque gain (k_t), x_2 as blade pitch angle (β), x can be given as $x = [x_1, x_2]^T$ and $\alpha \in (0, 1)$ gives weights on the two functions. The second assumption is that accurate measurements for rotor power, generator speed and structural load moments are available.

III. IMPLEMENTATION AND MULTI-VARIABLE CONTROLLER DESIGN

A. Implementation methodology

Real-time weighted, multi-variable, multi-objective optimization for wind turbines was implemented, as shown in Figure 3. For this study, power (P) is the objective to maximize and three different combination of load (L) objectives (to minimize) were evaluated: (i) $L = L_1(x_1, x_2)$ consisted of only the tower base fore-aft bending moment (TBFABM), (ii) $L = L_2(x_1, x_2)$ consisted of only the blade root flap-wise bending moment (BRFWBM), and (iii) $L = L_3(x_1, x_2)$ is a combination of TBFABM and BRFWBM with weights on each calculated based on multi-attribute decision theory (MADT) [11]. Under MADT, the weights included an additional cross-weighting term that addresses the effects of correlations/combinations between the two individual load moments. Overall, the load objective function for the combination case was given by

$$L_3(x_1, x_2) = k_1 L_1 + k_2 L_2 + (1 - k_1 - k_2) L_1 L_2 \quad (6)$$

where k_1 and k_2 are the appropriately calculated weights, and $(1 - k_1 - k_2)$ is the aforementioned cross-weighting term. Here, we derived these to be $k_1 = 0.73$ and $k_2 = 0.26$. These values were obtained based on hypothetical lottery scenarios over which the load moment in consideration will have substantial change [11]. It can be seen here that the cross-weighting term is almost negligible for our selected case.

From Figure 3, it can be seen that the objective functions power and load are first processed through a moving average filter of 12.5s. The power objective is then normalized with the rated turbine power, and its logarithm is fed to the gradient estimator. For the load objective, its running standard deviation is used, which is scaled with its running mean value and logarithm of the resultant is fed to the gradient estimator blocks. Note that for the combination case in (6), L_1 and L_2 are the normalized, non-dimensional tower base and blade root moments. The gradient estimator (GE) block is simply the high pass filter (HPF) $F_{HP}(s)$, the modulating signal and the low pass filter (LPF) $F_{LP}(s)$ as shown in Figure 4. The partial derivatives thus obtained are then concatenated to obtain the power and the load gradient vectors. These are then used to determine the optimizing weight α in real-time inside the multi-objective optimization (MOO) algorithm block.

In Figure 5, $\nabla P(x)$ is the power gradient vector, and $\nabla L(x)$ is the load gradient vector. The optimal α will yield

the minimum norm solution $\beta^* = \alpha \nabla P(x) + (1 - \alpha) \nabla L(x)$ (α thus obtained is optimal, as β would be the shortest length vector to the convex hull of the gradient vectors and hence least distance to the Pareto front). Therefore, the multi-objective weighting can be obtained in real-time through some trigonometric manipulations. The steps followed to determine the weight α is as below:

Step 1: Calculate $\cos \theta$ using dot product, where θ is angle between the two conflicting gradient vectors.

$$\cos \theta = \frac{\nabla P \cdot \nabla L}{\|\nabla P\| \|\nabla L\|} \quad (7)$$

Step 2: If $\|\nabla P\| = \|\nabla L\|$, α is set to 0.5.

Step 3: If $\cos \theta$ is between 0 and 1 (i.e., angle between two gradient vectors is acute), α is set to 1 if $\|\nabla P\| < \|\nabla L\|$ and if $\|\nabla L\| < \|\nabla P\|$, α is set to 0.

Step 4: Else the length z and d are calculated to obtain the weight $\alpha = \frac{z}{d}$.

B. Multi-variable ESC Parameter Design

ESC parameters were designed as discussed in [7]. The dither frequencies of both the ESC's were selected within the bandwidth of the plant dynamics. Rotor inertia and actuator dynamics corresponds to the input dynamics, output dynamics is reflected due to sensory dynamics and/or signal conditioning. To simplify, input and output dynamics are combined for parameter estimation from a open-loop step test responses under constant wind input. The step response of the rotor speed under step change in torque-gain and blade pitch indicates first-order dynamics. The estimated time constant from the torque-gain and blade pitch to the rotor speed is approximately 8s. The corresponding bandwidth of the combined input-output dynamic for the ESC is 0.125 rad/s. Dither frequency for both the torque gain ESC and the blade pitch ESC were selected within the estimated bandwidth. The Bode plots for the estimated plant dynamic and the filters in ESC design are shown in Figure 6. The low-pass and high-pass filters are first order filters. The ESC parameters are listed in Table I. Dither amplitude was selected, so that the dithered output has appropriate SNR at the dither frequency with respect to the section of output due to measurement noise, external disturbance and process variation.

The non-dimensional normalized torque gain introduced in [4], and later utilized in [12], is used here as the control parameter u . The optimal value of normalized torque gain is

$$u_{opt} = \frac{k_{opt}}{I_r} \times N^3 \approx 0.061 \quad (8)$$

where, $k_{opt} = 2.34 \text{ Nm}/(\text{rad/s})^2$ is the optimal generator torque gain for the NREL 5MW turbine, N is the gear ratio and I_r is the rotor inertia. The optimal generator torque control law is given by $\tau_g = k_{opt} \omega_g^2$, where ω_g denotes the generator speed. Optimal blade pitch angle for this turbine is $\beta_{opt} = 0^\circ$.

IV. RESULTS

The proposed logarithmic-feedback multi-objective optimization strategy for wind turbine region-2 control is

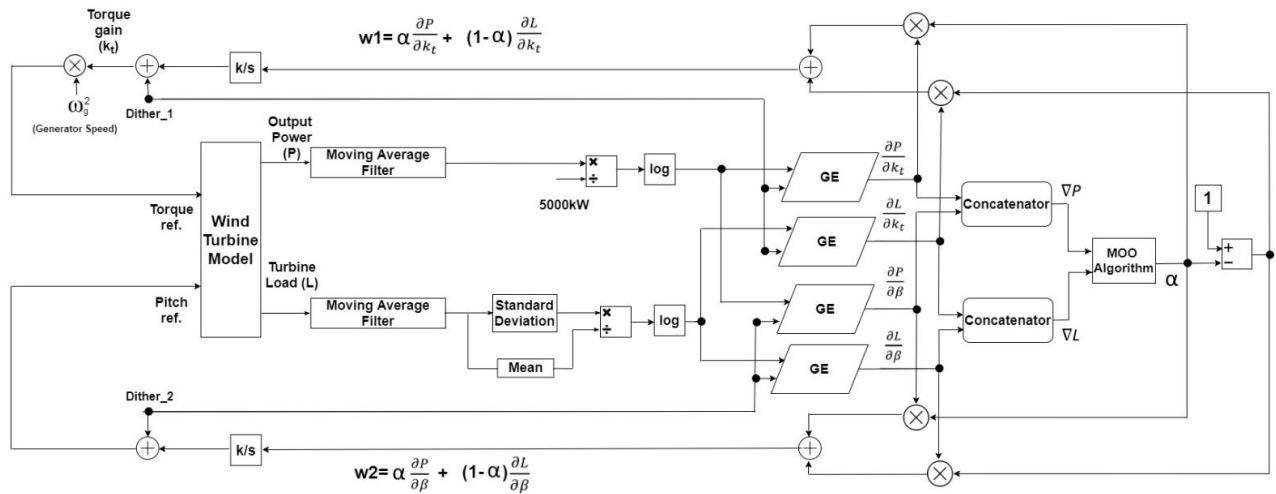


Fig. 3. Implementation of multi-objective ESC with log-feedback of power and loads.

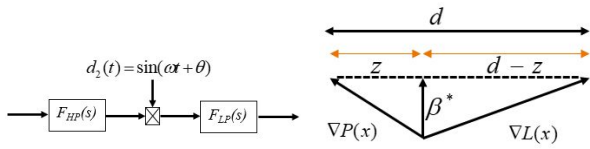


Fig. 4. Gradient estimator (GE).

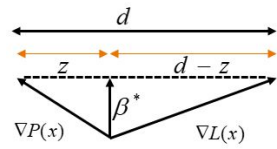


Fig. 5. Illustration of the position of minimum norm solution (β^*) with respect to the gradient vectors.

TABLE I
ESC PARAMETERS OF NREL 5MW REGION 2 CONTROLLER

Parameter	Torque-gain ESC	Blade-pitch ESC
Dither Frequency	0.02rad/s	0.04rad/s
Dither Amplitude	0.005 (non-dimensional)	0.4deg
Cut-off Freq. of LPF	0.015rad/s	0.015rad/s
Cut-off Freq. of HPF	0.018rad/s	0.018rad/s
Phase Compensator	0.36rad	0.209rad
Integrator Gain	0.00055/s	0.037/s

TABLE II
MAIN SPECIFICATIONS OF NREL 5MW TURBINE

Description	Value
Rating	5MW
Rotor diameter	126m
Cut-in, Rated, Cut-out wind speed	3m/s, 11.4m/s, 25m/s
Cut-in, Rated rotor speed	6.9RPM, 12.1RPM
Rotor Inertia	35444067kg.m ²

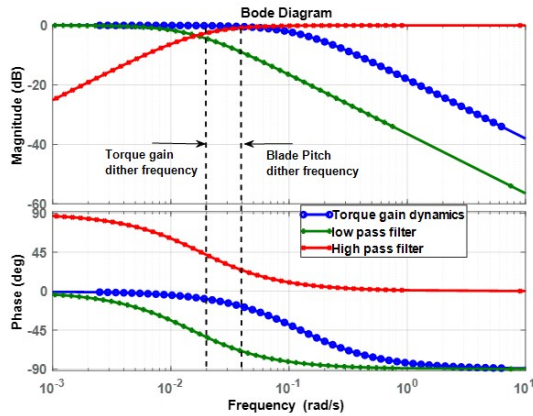


Fig. 6. Bode plots of input dynamics, LPF, HPF and the dither frequencies.

designed and simulated with the NREL 5MW reference turbine model in FAST. Main parameters of the turbine model are listed in Table II. The controllers are evaluated for hub-height mean wind speed of 9m/s, no wind shear and turbulent intensities (TI) of 10%, 15% and 20% respectively. Six different seeds were used to generate wind profiles for each turbulent intensity case in TurbSim, and then aggregate damage equivalent loads (DEL's obtained using MLife) are reported for comparison. Energy output was averaged over the six cases. ESCs were turned on at 150s. FAST simulations were performed first for the multi-variable (torque gain and blade pitch angle) single objective (power maximization)

ESC under different turbulent intensity wind profiles and then for the multi-variable, multi-objective ESC. All three combinations of load objectives discussed in Section III were evaluated. Percentage change is reported in terms of reduction in DEL's of multi-objective result with respect to the single objective result.

Figures 7 and 8 display the time series for torque gain, blade pitch, rotor power and rotor speed with load objective TBFBAM and 15% TI case. It can be observed that with multi-objective ESC, control inputs torque gain and blade pitch angle of the turbine operates in slightly sub-optimal conditions, with rotor speed lower than the optimal value such that the structural loads can be reduced. Time series for other TI and different feedback cases are not shown due to space limits.

Figure 9 displays the time series of the weight α assigned on the power objective, as well as the power and load gradient vectors, ∇P and ∇L , respectively. It can be observed that the cosine of the angle between the two gradient vectors is changing with time, and accordingly, the weight α is being

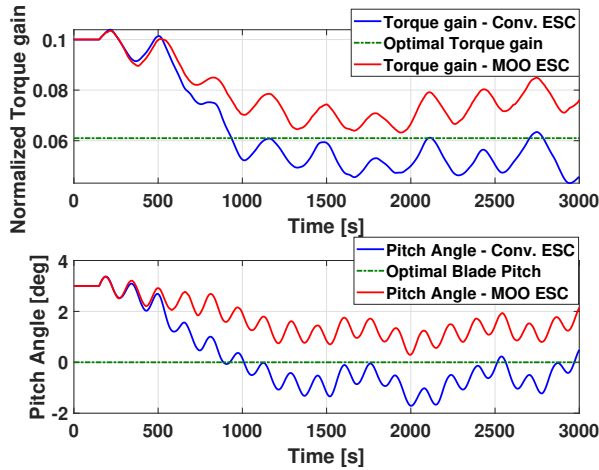


Fig. 7. Time series for torque gain and blade pitch with load objective TBFABM (9m/s, 15% TI wind).

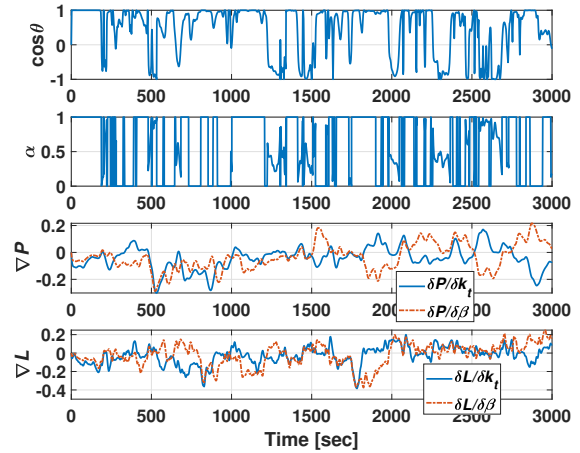


Fig. 9. Time series for multi-objective parameters with load objective TBFABM (9m/s, 15% TI wind).

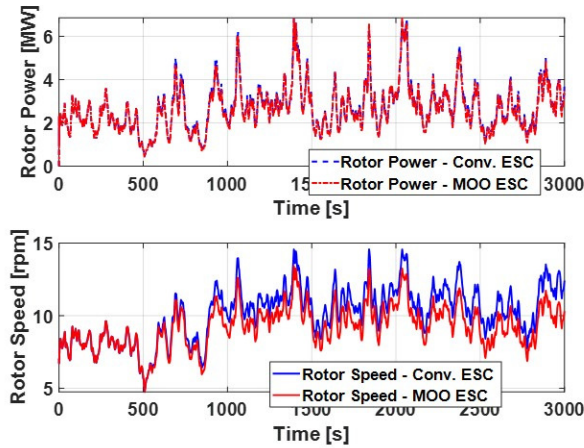


Fig. 8. Time series for rotor power and rotor speed with load objective TBFABM (9m/s, 15% TI wind).

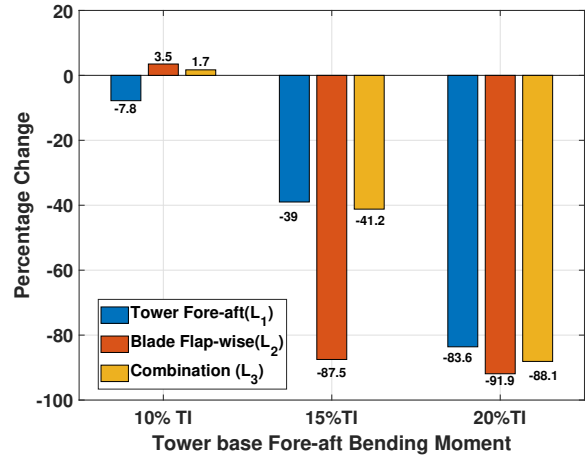


Fig. 10. DEL change in tower base fore-aft bending moment.

modified in real time for faster convergence to the Pareto front.

Figure 10 shows the change in tower-base fore-aft bending moment (TBFABM) DEL, while Figure 11 shows the DEL percentage change in blade root flap-wise bending moment (BRFWBM). The average percentage change in energy production is shown in Figure 12. All three controllers (for each load objective) are evaluated. All metrics are calculated for three values of turbulence intensity (TI). Averaging these results across all three TIs, we obtain the aggregate change in loads and energy shown in Table III.

Preliminary conclusions can be drawn from Table III. Firstly, note that if one assumes the same level of interest in reducing both loads (blade and tower), the controller with tower-load feedback (TBFABM feedback) performs as well as the controller with blade-load feedback (BRFWBM feedback), but both the controllers have a lower average total load reduction (row 3 in Table III) than the controller with combined load feedback. In this case, one would select the

combined load feedback controller, which has the largest average load reduction and energy loss (1.8%) approximately the same as the best possible energy loss (1.7%). One point to consider here would be if only tower-load feedback is used, then only one sensor on the tower would be required in comparison to two sensors (one on tower and one on blade) for the combined feedback case. Note from Table III that the combined load feedback controller attains the largest blade DEL reduction (87%); hence, this controller is the best choice even if we only care about reductions in blade DEL. One would select the blade-load feedback controller if the target is to reduce tower DELs only, because this controller achieves the largest tower DEL reduction (59%). However, based on this metric alone, this controller is about 34% better than the tower-feedback controller and about 37% better than the combined load feedback controller. Given all the uncertainties associated with this analysis, the use of blade-load feedback may not be justified.

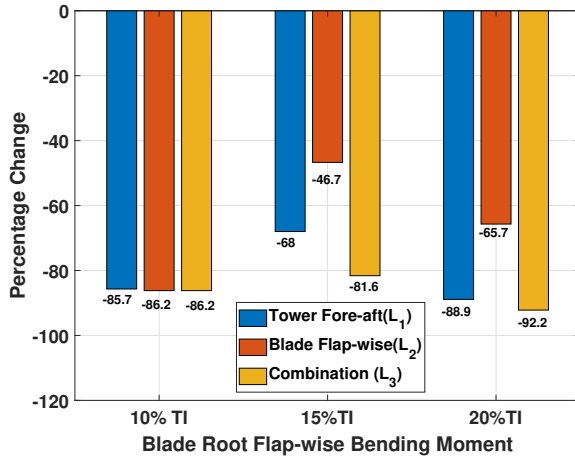


Fig. 11. DEL change in blade root flap-wise bending moment.

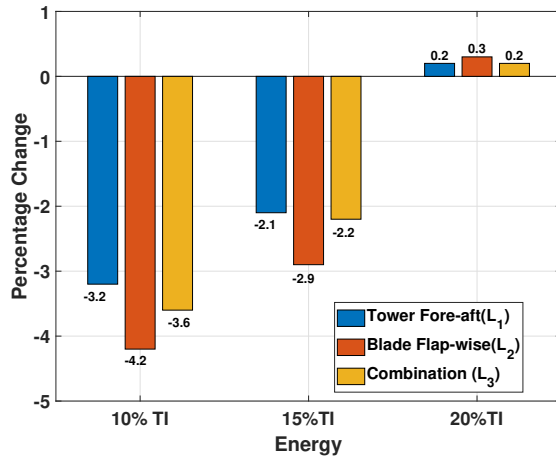


Fig. 12. Change in energy capture.

V. CONCLUSION

This paper proposes a real-time weighted multi-objective ESC with log-feedback strategy for wind turbine control. The proposed multi-objective strategy is compared with a conventional single objective (power maximization) ESC strategy. The 5MW NREL reference turbine model is used to evaluate the performance of both strategies. Three different load objectives are considered: tower fore-aft bending moment, blade-root flapwise bending moment and a combination of both. Preliminary results demonstrate that the proposed method converges to solutions with much greater load reductions than the change in energy capture. That is, the inclusion of load objectives in this multi-objective ESC configuration reduces loads with little to no impact on energy capture. From the limited analysis, it can be concluded that the multi-objective ESC controller with log-feedback of power and combined load of tower and blade offers the best compromise in terms of performance, but it requires two sensors. For simplicity, load feedback of tower would be the best option.

TABLE III
AVERAGE CHANGE IN LOADS AND ENERGY FOR THE THREE LOAD OBJECTIVES

	TBFABM feedback (L_1)	BRFWBM feedback (L_2)	Combined feedback (L_3)
TBFABM DEL Change(%)	-44	-59	-43
BRFWBM DEL Change(%)	-81	-66	-87
Average DEL Change(%)	-62.5	-62.5	-65
Energy(%)	-1.7	-2.3	-1.8

The algorithm presented for multi-objective optimization (see Fig. 3) does not require the design of weights for the individual objectives. Instead, such weights are calculated in real-time, resulting in an algorithm that appears to converge to the Pareto optimal solution that is closest to the initial condition for the optimization variables. Additional work is required to determine the convergence properties of the proposed algorithm.

REFERENCES

- [1] L. Y. Pao and K. E. Johnson, "Control of wind turbines," *IEEE Control Systems*, vol. 31, pp. 44–62, 2011.
- [2] J. Creaby, Y. Li, and J. E. Seem, "Maximizing wind turbine energy capture using multivariable extremum seeking control," *Wind Engineering*, vol. 33, no. 4, pp. 361–387, 2009. [Online]. Available: <https://doi.org/10.1260/030952409789685753>
- [3] Y. Xiao, Y. Li, and M. A. Rotea, "Cart3 field tests for wind turbine region-2 operation with extremum seeking controllers," *IEEE Transactions on Control Systems Technology*, pp. 1–9, Apr 2018.
- [4] M. A. Rotea, "Logarithmic power feedback for extremum seeking control of wind turbines," *IFAC-PapersOnLine*, vol. 50, no. 1, pp. 4504 – 4509, 2017, 20th IFAC World Congress.
- [5] U. Ciri, S. Leonardi, and M. A. Rotea, "Evaluation of log-of-power extremum seeking control for wind turbines using large eddy simulations," *Wind Energy*, vol. 22, no. 7, pp. 992–1002, 2019. [Online]. Available: <https://onlinelibrary.wiley.com/doi/abs/10.1002/we.2336>
- [6] Y. Xiao, Y. Li, and M. A. Rotea, "Multi-objective extremum seeking control for enhancement of wind turbine power capture with load reduction," *Journal of Physics: Conference Series*, vol. 753, p. 052025, sep 2016.
- [7] M. A. Rotea, "Analysis of multivariable extremum seeking algorithms," in *Proceedings of the 2000 American Control Conference. ACC (IEEE Cat. No.00CH36334)*, no. 6, 2000, pp. 433–437, vol. 1.
- [8] M. A. Rotea, "Method and system for using logarithm of power feedback for extremum seeking control," US Patent App. 16/617,911, 2020.
- [9] S. Kumar and N. Gans, "Extremum seeking control for multi-objective optimization problems," in *2016 IEEE 55th Conference on Decision and Control (CDC)*, 2016, pp. 1112–1118.
- [10] J.-A. Désidéri, "Multiple-gradient descent algorithm (mgda)," INRIA, Research Report RR-6953, June 2009.
- [11] R. T. Clemen and T. Reilly, *Making hard decisions with Decision Tools*. Cengage Learning, 2013.
- [12] D. Kumar and M. A. Rotea, "Log-power PIESC for wind turbine power maximization below-rated wind conditions," in *AIAA Scitech 2021 Forum*, January 2021, pp. 1–10. [Online]. Available: <https://arc.aiaa.org/doi/abs/10.2514/6.2021-1288>